

Intensified optical camera with Timepix4 readout

Erik Hogenbirk^a Andrei Nomerotski,^{b,c,d} Bram Bouwens,^a Gabriel Diaz,^a Shazia Farooq,^a Sergei Kulkov,^b Erik Maddox,^a Ondrej Matousek,^b Peter Svihra,^{b,d} Henrique Zanolia^a

^a*Amsterdam Scientific Instruments, Science Park 106, 1098 XG, Amsterdam, The Netherlands*

^b*Faculty of Nuclear Sciences and Physical Engineering, Czech Technical University in Prague, Břehová 7, Prague, Czech Republic*

^c*Department of Electrical and Computer Engineering, Florida International University, 10555 West Flagler St, Miami, U.S.A*

^d*Institute of Physics of the Czech Academy of Sciences, Na Slovance 1999/2, Prague, Czech Republic*

E-mail: andrei.nomerotski@cvut.cz

ABSTRACT: We report the first characterization results of an optical time-stamping camera based on the Timepix4 chip coupled to a fully depleted optical silicon sensor and fast image intensifier, enabling sub-nanosecond scale, time-resolved imaging for single photons. The system achieves an RMS time resolution of 0.3 ns in direct detection mode without the intensifier and from 0.6 to 1.5 ns in the single-photon regime with an intensifier for different amplitude-based signal selections. This shows that Timepix4 provides a significant improvement over previous Timepix3-based cameras in terms of timing precision, and also in pixel count and data throughput. We analyze key factors that affect performance, including sensor bias and timewalk effect, and demonstrate effective correction methods to recover high temporal accuracy. The camera's temporal resolution, event-driven readout and high rate capability make it a scalable platform for a wide range of applications, including quantum optics, ultrafast imaging, and time-correlated photon counting experiments.

KEYWORDS: fast optical camera, Tpx3Cam, timewalk calibration, Timepix3, Timepix4

ARXIV EPRINT: [2509.14649](https://arxiv.org/abs/2509.14649)

Contents

1	Introduction	1
2	Methods	2
2.1	Timepix4 readout chip	2
2.2	Optical Timepix cameras	3
2.3	Optical setup	3
3	Results	3
3.1	Non-intensified camera	4
3.2	Intensified camera	5
3.3	Timewalk correction	5
3.4	Time resolution	6
3.5	Dependence on bias voltage	7
4	Conclusions	8

1 Introduction

The ability to detect, count, and time-stamp individual optical photons is becoming increasingly important across a wide range of imaging applications. This approach enables the capture of the complete spatio-temporal and, in principle, also spectral information carried by each detected photon, providing deeper insight into the underlying physical processes. Photon-counting is already well established in X-ray imaging, where sufficient photon energy allows for direct detection and time-resolved, energy-resolved measurements. High-rate readout electronics further enable rapid accumulation of statistics, making this modality highly efficient for quantitative imaging.

In the optical domain, the development of time-stamping cameras — particularly those based on the Timepix family readout chips — has enabled similar capabilities for visible and near-infrared photons [1, 2]. These systems offer nanosecond-scale timing resolution, opening new avenues in areas such as ion imaging [3–6], optical readout of time-projection chambers (TPC) [7], fluorescence lifetime imaging [8–10], neutron detection [11–14] and quantum sciences [15–24]. Timepix-based single photon sensitive cameras with direct registration of MCP electrons with the Timepix ASIC metal pads have been also developed and tested [25–27].

In applications that require single-photon detection, this sensitivity is achieved by coupling the camera to an image intensifier that employs a fast (typically P47 type) scintillator. This allows detection of individual optical photons with high spatial and temporal precision. As a result, time-stamping optical cameras, such as Tpx3Cam (also known as Chronos Phoebe from ASI), have emerged as a versatile platform for investigating low-light, time-resolved, and photon-statistical phenomena in both fundamental research and applied science. The timing resolution is one of the most important figures of merit for the time-stamping cameras. Here we describe the first tests of an intensified optical Timepix4 camera, focusing on its superior timing resolution compared to the previous version of the camera with the Timepix3 chip [2].

There are several types of imaging cameras capable of single-photon detection, e.g., intensified time-stamping complementary metal-oxide-semiconductor cameras (iCMOS) [28], intensified or electron-multiplying charge-coupled device cameras (iCCD or EMCCD) [29–35], cameras based on direct registration of charge generated by micro-channel plates (MCP) in Timepix chips [25, 36] and resistive anodes (PhotonPix™ camera) [37]; and cameras based on single-photon avalanche diodes (SPADs) [38–45]. We refer the readers to existing reviews of the subject [46–48].

2 Methods

For the tests described here, we developed an optical camera based on the Timepix4 chip bump-bonded to a silicon sensor that is adapted for optical photons. This sensor is identical to the one used in optical cameras based on Timepix3. A housing with a C-mount flange ensures that an intensifier or lenses can be correctly mounted and focused.

The testing was performed with a pulsed blue 450 nm laser that illuminated a small area of the optical Timepix4 camera field of view. This was done both for intensified and non-intensified camera configurations. The timing studies relied on measurements of a delay between the laser pulse and the time-stamped pixel response. The experimental setup is schematically shown in the left part of Figure 1, and we describe it and its essential components below.

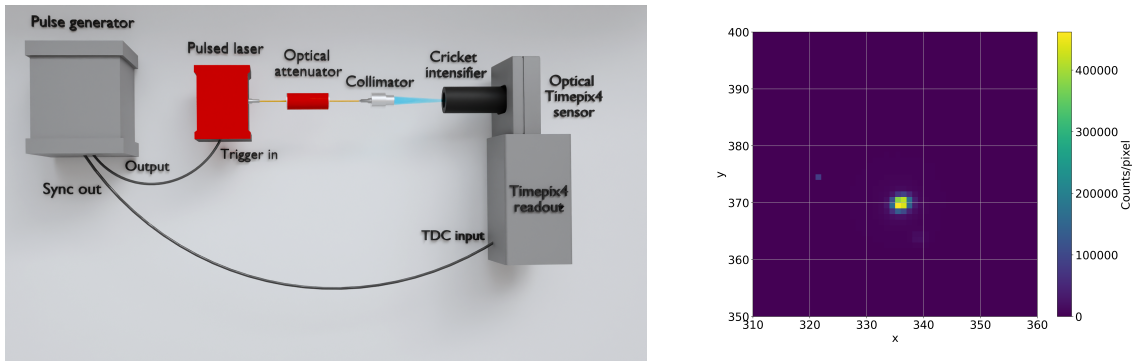


Figure 1. Left: Experimental setup with intensified camera and 450 nm laser with pulse duration of 90 ps, triggered with a pulse generator running at 185 kHz. The fiber-coupled light flash had provisions to be attenuated before collimation onto the camera. The measurements have been performed with and without an intensifier, but only the intensified configuration is shown here. Right: the camera (x,y) occupancy map in configuration with an intensifier for a focused beam.

2.1 Timepix4 readout chip

The Timepix4 is a next-generation pixel readout chip developed by the Medipix4 collaboration, designed for high-resolution, time-resolved particle and X-ray detection [49]. It features a matrix of 512×448 pixels with a $55 \mu\text{m} \times 55 \mu\text{m}$ pixel pitch, and offers simultaneous measurement of time-of-arrival (ToA) and time-over-threshold (ToT) per pixel. The chip supports data-driven readout and multi-hit capability, enabling each pixel to independently report events without the need for a global trigger, which is critical for sparse, high-rate environments [50]. Its back-end architecture supports hit rates exceeding $180 \text{ Mhit/cm}^2/\text{s}$, making Timepix4 well-suited for high-throughput, time-resolved imaging. Timepix4 measures time with a granularity of 195 ps corresponding to an RMS resolution of about 60 ps. For comparison, the Timepix3 time bin size is 1.56 ns, corresponding to a time resolution limit of 450 ps.

2.2 Optical Timepix cameras

Optical cameras based on the Timepix3 chip have become a powerful tool for time-resolved photon detection in the visible and near-infrared domains used in a multitude of applications. The Timepix3 chip features a data-driven readout architecture, enabling each of its 256×256 pixels (with $55 \mu\text{m}$ pitch) to independently record both the time-of-arrival (ToA) and time-over-threshold (ToT) of incoming signals with a timing resolution of 1.56 ns and some energy discrimination via pulse-height ToT information [51].

In optical imaging applications, these cameras are typically coupled to optical sensors with high quantum efficiency in the 400-950 nm wavelength range [52]. Threshold for time-stamping a fast light flash is about 1000 photons per pixel [2]. The optical data-driven time-stamping concept was originally developed in 2015 for ion imaging in the velocity map imaging (VMI) applications when the first optical sensors compatible with the Timepix chip had been developed and produced [1]. For single-photon applications, image intensifiers are employed, which convert single photons into fast light flashes that can be detected by the optical sensor with high efficiency. This configuration enables single-photon sensitivity, nanosecond timing, and spatial resolution within the same platform. Since the intensifier and camera are completely mechanically decoupled, the same camera can be used with different intensifiers and detection schemes, which makes this configuration particularly flexible.

The first single-photon-sensitive Timepix camera was used for lifetime imaging in 2017 [8], and the intensified Timepix3 camera was first tested for quantum applications in 2019 [15]. At present, optical Timepix3 cameras are increasingly used in fields such as quantum optics, ion and electron imaging, fluorescence lifetime imaging, and time-resolved spectroscopy, where precise spatio-temporal characterization of low-light signals is essential. Their ability to operate in event-driven mode without the need for external triggering makes them particularly well-suited for detecting sparse, asynchronous photon events with minimal dead time.

In the optical Timepix4 camera used for these experiments, a Timepix3 optical sensor, which is smaller in area than the full Timepix4 chip, was bump-bonded to Timepix4 and read out with SPIDR4 electronics. The leakage current of the sensor was larger than usual, which is likely caused by the edges of the sensor touching parts of the Timepix4 solder bump array. We therefore kept the bias voltage limited to 70 V in the experiments, while typically it can be safely increased to 100 V. The camera had mounting provisions for the image intensifier packaged as Photonis CricketTM, which integrates the intensifier, power supply, and back-end optics between the intensifier output and optical sensor. The camera also implements up to four time-digital-converters (TDC) employing some of the peripheral Timepix4 pixels for precise time-stamping of external signals. We employed it to time-stamp the pulse generator synchronization signal used to trigger the 90 ps laser flash.

2.3 Optical setup

The 450 nm laser (Thorlabs GSL45A) was triggered with a pulse generator at 185 kHz. The laser pulse had the minimal allowed pulse duration of 90 ps. The produced light flash had provisions for attenuation before collimation onto the camera. In practice, the attenuation was used only in configuration with the intensifier. The right half of Figure 1 shows the camera (x,y) occupancy map with the intensifier for a well-focused beam.

3 Results

The primary goal of this study was to evaluate the achievable time resolution for the Timepix4 camera in optical configurations. The key question here would be to quantify the improvement of

temporal resolution due to the improved time binning of the readout chip, from 1.56 ns in Timepix3 to 195 ps in Timepix4, so an improvement by a factor of eight. However, it is not clear at all if this improvement can be realized as the signal amplification in the intensifier involves light emission of the P47 scintillator, which may limit the achievable resolution improvement due to its relatively slow time response with risetime of 7 ns [53]. The study below is the first attempt to quantify this effect.

3.1 Non-intensified camera

First we performed tests of the optical Timepix4 camera without the intensifier. In this configuration the camera is not single-photon sensitive, but detection can be achieved by a sufficiently bright flash. After adjusting the focusing a small spot corresponding to several pixels was illuminated on the sensor. We selected a single pixel in this spot, and all results presented below were obtained for this single pixel, so we did not need to account for the pixel-to-pixel variability issues. We assumed and relied on the previous experience that the pixel behaviour is uniform enough across the chip.

The blue light with the wavelength of 450 nm is absorbed near the surface in silicon with an absorption depth of about 0.5 micron. The produced carriers (holes as the sensor is p-on-n type) need to drift through the full thickness of the depleted sensor to the Timepix4 pixels. The drift time would depend on the applied bias voltage and possibly on the properties of the surface, which may require additional bias voltage to be fully depleted. Diffusion of the drifting holes may affect the time resolution at 100 ps level, but it is not expected to contribute significantly to the time resolution.

The left part of Figure 2 shows the distribution of measured distances between consecutive TDC synchronization pulses fit with a Gaussian function. The temporal jitter of a single laser pulse can be estimated as $0.13 \text{ ns}/\sqrt{2} = 0.09 \text{ ns}$, demonstrating excellent stability of the laser reference signal. The measured period of 5405 ns agrees with the laser pulsing frequency of 185 kHz. The right part of Figure 2 shows the two-dimensional distribution of time differences between the laser synchronization signal and ToA of one of the hit Timepix4 pixels activated with a flash of light from the laser versus the pixel ToT. We see that the ToT of the used pixel is contained in the 3500-3800 ns range and so does not vary much. We note that this value is due to direct illumination of the pixel during a single 90 ps laser flash.

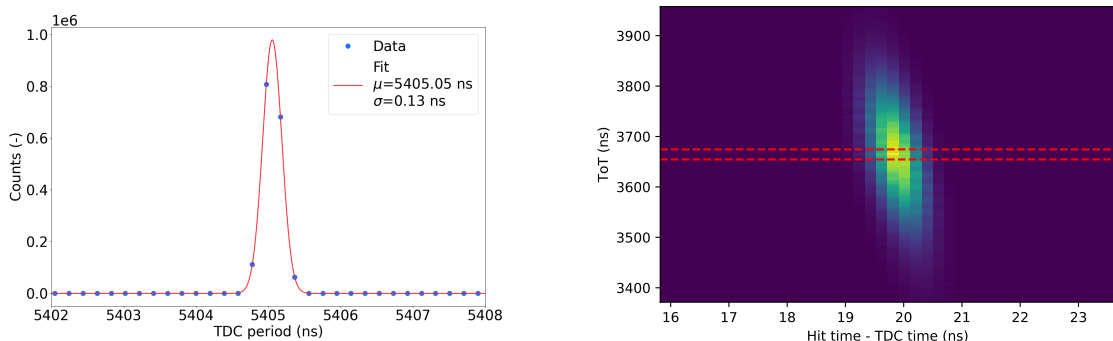


Figure 2. Left: Distribution of measured distances between consecutive TDC pulses demonstrating the laser stability; Right: Two-dimensional distribution of time differences between the laser synchronization signal and ToA of one of the hit Timepix4 pixels versus the pixel ToT. The pixels were activated with a direct flash of light from the laser.

The left part of Figure 3 shows the time difference distribution for a pixel activated with a flash of light from the laser without any TOT selection, while the right graph shows the same but with TOT selection in a 25 ns slice indicated with red dashed lines in Figure 2. The time resolution (RMS) was estimated by fitting the Gaussian function to the time difference distribution. The resolution was equal to 318 ps for the whole dataset and to 272 ps for a selected 25 ns slice of ToT values. The measurements were performed at a bias voltage of 50 V.

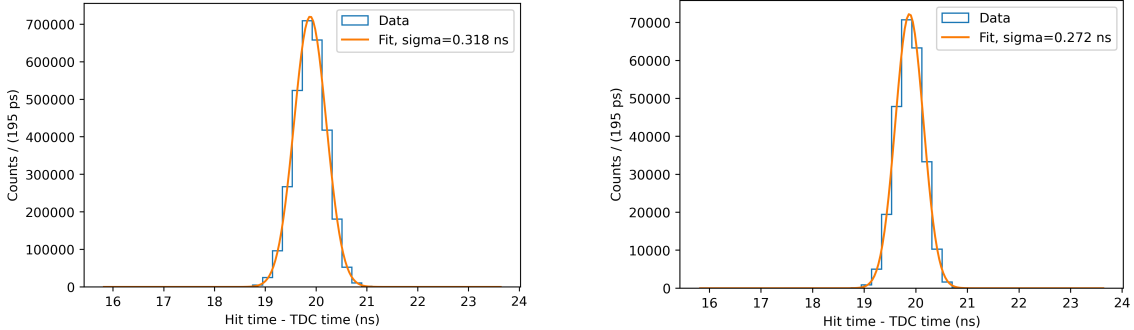


Figure 3. Left: Distribution of time differences between the laser synchronization signal and ToA of one of the hit Timepix4 pixels without any TOT range selection. Right: Distribution of time differences between the laser synchronization signal and ToA of one of the hit Timepix4 pixels with TOT selection in a 25 ns slice shown in Figure 2 (right). The measurements were performed at a bias voltage of 50 V.

3.2 Intensified camera

We used the intensifier from Photonis with a hi-QE-blue photocathode, chevron (double-layer) MCP at its maximum gain of about 10^6 , and P47 scintillator. The intensifier was used in the CricketTM configuration with the laser flash directed to the intensifier photocathode. In this case, the laser pulse had to be strongly attenuated to provide a reasonable rate of single photons. The typically activated area of several pixels is shown in the right part of Figure 1.

The P47 scintillator emits light over a spectrum with a maximum at 430 nm and an approximate range of 390-490 nm [53], and, thus, it behaves similarly, in terms of photon absorption, to the used 450 nm laser with photon conversions near the silicon sensor surface and considerable drift time through the full sensor depth. The left part of Figure 4 shows the two-dimensional distribution of time differences between the laser synchronization signal and ToA of one of the Timepix4 pixels versus ToT. The measurements were performed at a bias voltage of 70 V. The distribution clearly shows the expected dependence of the delay on ToT due to the timewalk effect, addressed in detail in the following section. As an example of time resolution value we estimate it for ToT selection in the range of 2000-2200 ns, as shown in the right part of Figure 4, to be equal to 0.83 ns. This demonstrates that we can achieve sub-nanosecond resolution for the intensified (and so single-photon sensitive) optical Timepix4 camera if the intensifier gain is large enough, see further discussion in Section 3.4.

3.3 Timewalk correction

The timewalk terminology is used to describe the dependence of the timing response on the signal amplitude. For linear discriminators such as used in Timepix4 pixels with larger signals cross the threshold earlier than signals with smaller amplitudes. This effect can be studied and corrected for as previously demonstrated with both Timepix3 and Timepix4 chips [3, 54, 55].

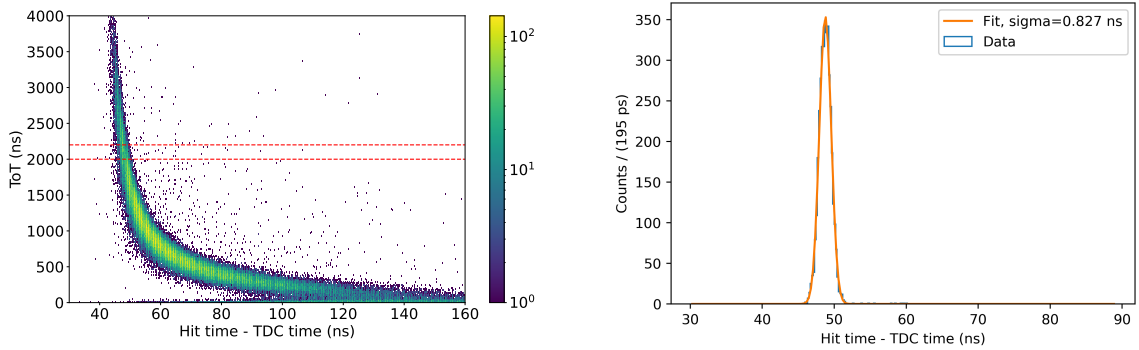


Figure 4. Left: Distribution of ToT versus time difference between the laser and pixel. The TOT selection in a 200 ns range, from 2000 to 2200 ns, is indicated with red dashed lines. Right: Distribution of time differences between the laser synchronization signal and ToA of one of the hit Timepix4 pixels with TOT selection in a 200 ns range fit with a Gaussian function. The measurements were performed at a bias voltage of 70 V.

We performed timewalk correction by fitting the time difference distributions with a Gaussian function in 92.5 ns slices of ToT. Figure 5 shows the results of the fit for the mean values as a function of ToT in the left part of the figure. The mean values are marked with red dots on the top of the time difference versus the ToT distribution. The right part of the figure shows the two-dimensional distribution of time difference versus ToT after the timewalk correction. The measurements were performed at a bias voltage of 70 V. One can see that the timing jitter is larger for smaller values of ToT, even after the timewalk correction.

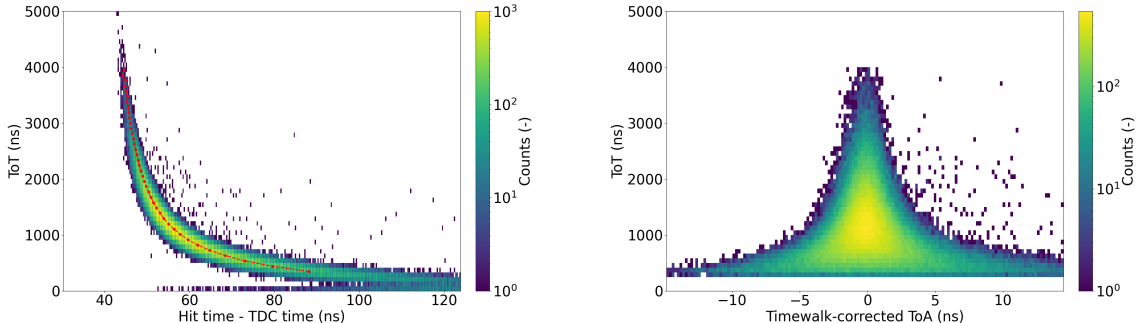


Figure 5. Left: results of the Gaussian fit for the mean values as a function of ToT. The mean values are marked with red dots on the top of the time difference versus the ToT distribution. Right: time difference distribution versus ToT after the timewalk correction.

3.4 Time resolution

Evaluation of the timewalk correction requires performing Gaussian fits of the ToT slices. The left part of Figure 6 shows the fit results for the sigma values as a function of ToT. Distributions of time differences are explicitly shown in inserts for the last three points with the highest ToT values. We note that the timing resolution for these ToT values is around 600-700 ps, which is very good indeed, also meaning that other contributing factors to the resolution, such as surface charge collection, diffusion in silicon and scintillator response, are under control and below this value.

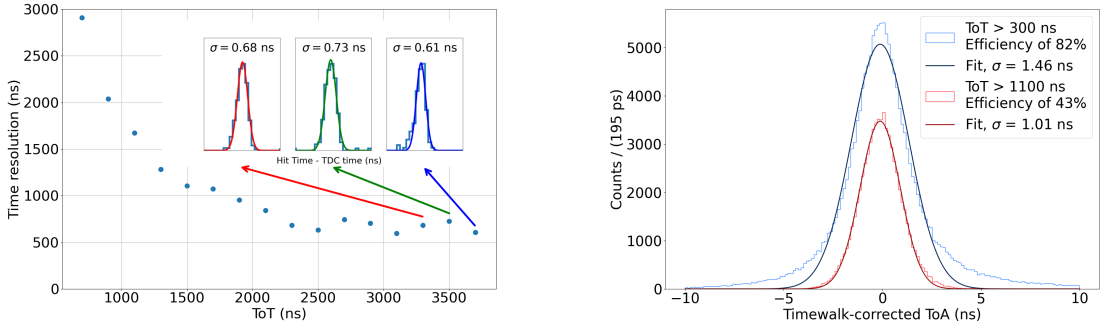


Figure 6. Left: Results of the Gaussian fit for the sigma values as a function of ToT. The distribution of time differences is explicitly shown in inserts for three points with the highest ToT values. Right: Two time difference distributions after the timewalk correction, selecting ToT larger than, respectively, 300 ns and 1100 ns, fit with Gaussian functions.

After the timewalk correction, the entire time difference distribution was fit with a Gaussian function, selecting ToT larger than 300 ns, which accounted for 83% of events. The fit is shown in the right part of Figure 6, resulting in time resolution of 1.46 ns. The same procedure with 1100 ns ToT selection yields the resolution of 1.01 ns and efficiency of 43%. For this study, we used the cluster based information, where ToA of the brightest pixel in the cluster is used as an estimate of the single photon time-stamp. The cluster is a collection of adjacent pixels, defined during data post-processing, which effectively represents the detector response to a single photon [2].

The ToT distribution is covering a wide range from small to large ToT values due to substantial gain variations of the MCP response to photoelectrons, which is characteristic of any intensifier. The largest ToT values in the intensified case, presented in this section, reach the ToT range of the non-intensified case and, therefore, the time resolution of 600-700 ps achieved there can be directly compared to 272 ps in the non-intensified case in the right part of Figure 3. It is likely that the difference in the resolution between these two cases can be explained primarily by the P47 scintillator contribution; we reckon that other possible contributions from the photocathode-to-MCP transit and in MCP itself are considerably smaller. We consider this as a viable confirmation that there are no fundamental showstoppers for the intensified optical Timepix4 cameras to deliver the time resolution around 600 ps if the optical gain is high enough.

3.5 Dependence on bias voltage

Photons emitted by the P47 scintillator in the intensifier are converted to photoelectrons near the sensor surface. Charge collection from the surface depends on the depletion of silicon in this area and, therefore, depends on the applied bias voltage. We measured the dependence of the collection time behaviour on the bias voltage by acquiring datasets for six different voltages: 20, 30, 40, 50, 60, and 70 V in the configuration with an intensifier. Figure 7 shows the ToT versus time difference distributions and individual time difference distributions for all values of the bias voltage. We see that the measured time difference decreases from over 100 ns values for a bias of 20 V when the sensor should start to be fully depleted to the values around 50 ns for a maximum bias voltage of 70 V. The latter delay includes the drift time through 300 micron of depleted silicon and additional time offset between the signals. In all cases the timewalk effect is clearly visible. The time difference distributions in the right part of Figure 7 were selected with ToT in the 2000 - 2200 ns range indicated with red lines in the left part of the figure.

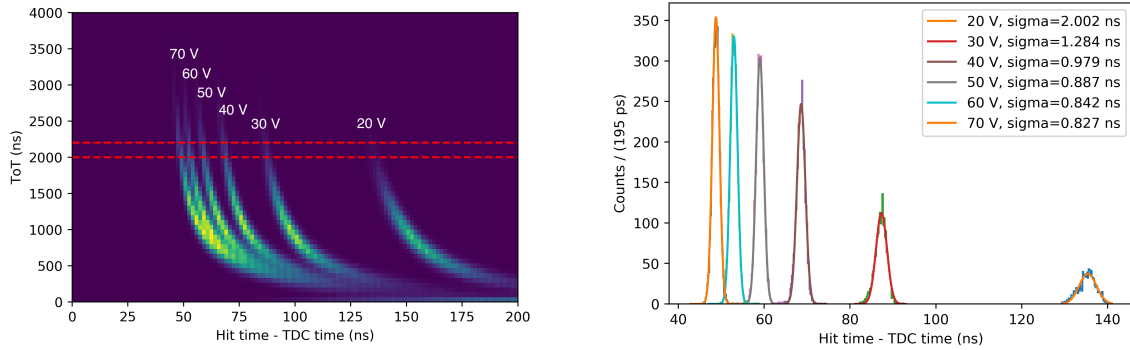


Figure 7. Left: Distribution of ToT versus time difference for multiple values of the bias voltage for the intensified configuration. Right: Distribution of time difference for multiple values of the bias voltage.

The left and right panels of Figure 8 present, respectively, the time delay between the laser synchronization signal and the ToA of a single Timepix4 pixel activated by a laser flash, and the corresponding time resolution as a function of bias voltage, both obtained with a ToT selection in a 200 ns window from 2000 to 2200 ns. Assuming the variation in delay with applied voltage V is entirely caused by the changing drift velocity of the holes through the sensor, we can describe the dependence as

$$\Delta t = \left(\frac{d^2}{\mu_h} \right) \frac{1}{V} + t_0 \quad (3.1)$$

with d the sensor thickness, t_0 the constant offset due to other effects and μ_h the hole mobility. This function is fitted to the delay in the left part of Figure 8, yielding a mobility of $(3.7 \pm 0.2) \times 10^2 \text{ cm}^2 \text{V}^{-1} \text{s}^{-1}$, which is in good agreement with literature values at temperatures slightly above room temperature [56] and thus confirming that the measured delay can be explained by the drift of holes in depleted silicon.

The time resolution for the ToT selections, as shown in the right part of Figure 8, reaches 0.83 ns at 70 V and remains better than 1 ns for a bias voltage as low as 40 V. These results indicate that the ultimate timing performance of the intensified optical camera with Timepix4 readout can be probed at higher bias voltages, which enable prompt charge carrier collection, and at the highest achievable ToT values, which minimize the impact of timewalk corrections and their associated jitter.

An interesting observation is also that the time resolution exhibits a dependence on the applied bias voltage even for identical ToT values. This behavior suggests that the sensor-related effects, such as, for example, increased time jitter arising from charge diffusion during carrier drift in the depleted silicon region might play a role at the lower bias voltages.

4 Conclusions

Timepix3 and Timepix4 are both hybrid-pixel, event-driven readout chips that, when coupled to an optical sensor and image intensifier, enable single-photon, time-resolved optical imaging. Timepix3 provides a 256×256 array (55 μm pitch), 1.56 ns time-of-arrival (ToA), and per-pixel time-over-threshold (ToT). Timepix4 enlarges the matrix to 512×448 at the same pitch (3.5 \times area), improves ToA binning to 195 ps, and sustains considerably higher hit rates. Both output ToT, but Timepix4's upgraded front-end yields more accurate amplitude estimates. Overall, Timepix4 offers superior timing, throughput, and scalability for high-flux, sub-nanosecond optical experiments.

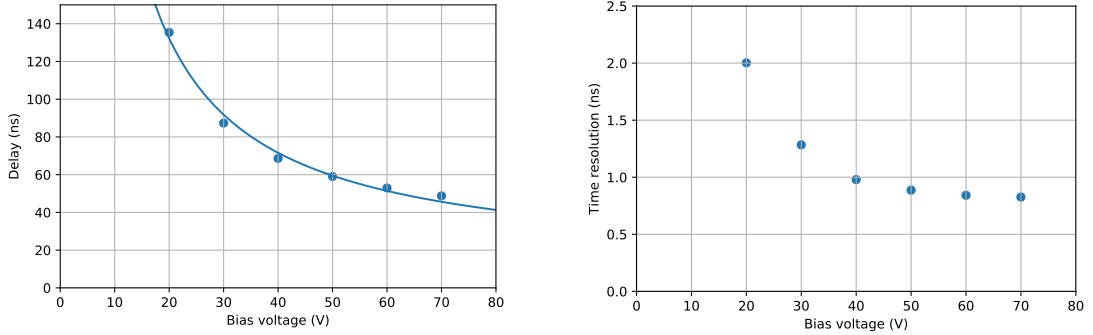


Figure 8. Left: Time delay between the laser synchronization signal and ToA of one of the hit Timepix4 pixels as a function of bias voltage. The pixel is activated with a flash of light from the laser with TOT selection in a 200 ns slice. Right: Measured time resolution with TOT selection in a 200 ns slice as a function of bias voltage. The 2000-2200 ns ToT slice is indicated with red lines in Figure 7.

Table 1 presents a comparison of timing resolutions (RMS) achieved in this study for different configurations of the Timepix4 camera. The resolution deteriorates after the addition of the intensifier, mostly due to the appearance of a scintillator as an intermediate step in the amplification chain. The P47 scintillator typically used in fast image intensifiers has a rise time of about 7 ns and, therefore, can limit the time resolution in situations with insufficient gain. Faster scintillators are becoming available [53, 57], which can be used in intensifiers and also for similar MCP-based amplification schemes employed for ion and electron detection. Another opportunity to increase the signal amplitude with the aim of improving time resolution is to employ optical sensors based on low-gain avalanche diodes (LGAD), which typically provide a gain of 5 to 10 [58–60]. Work is in progress to implement and evaluate these options.

Table 1. Timing resolution (RMS) achieved for the optical Timepix4 camera in different configurations.

Configuration	Time resolution [ns]	Comments
direct flash: no ToT selection	0.32	ToT range 300 ns
direct flash: ToT selection	0.27	ToT range 25 ns
intensifier: mild ToT selection + timewalk correction	1.0–1.5	large detection efficiency
intensifier: high ToT selection	0.6–0.7	small detection efficiency

In summary, we presented the first characterization of an optical camera based on the Timepix4 chip coupled to an optical silicon sensor and image intensifier, demonstrating its potential for sub-nanosecond scale, time-resolved single-photon imaging. The system achieved time resolutions down to about 0.3 ns without the intensifier and as low as 0.6 ns with the intensifier in the single-photon regime and selection of signals with high amplitude. For two more inclusive cases of amplitude selections covering, respectively, 43% and 83% of events, the resolutions with the intensifier are equal to 1.0 ns and to 1.5 ns, which is still a factor of two to three better than the resolution achieved in the past with Timepix3 cameras [2, 3]. These measurements validate the capability of the Timepix4-based optical cameras to perform fast, high-resolution optical time-stamping. The observed performance marks a significant improvement over previous Timepix3-based systems, particularly in terms of timing precision, pixel count, and readout rate.

Our results also highlight key factors influencing timing performance, including the sensor

bias voltage, intensifier scintillator properties, and timewalk effects. After applying a timewalk correction and optimizing selection criteria, we demonstrated sub-nanosecond timing with intensified readout - a performance level suitable for single-photon imaging in quantum optics, ultrafast imaging, and time-correlated photon counting experiments. With its high throughput and improved timing resolution, the Timepix4 camera is well positioned as a scalable platform for next-generation time-resolved optical measurements across a broad range of scientific domains.

Acknowledgments

This research was supported by the Czech Science Foundation (GACR) under Project No. 25-15534M and Czech Ministry of Education, Youth and Sports Project No. LM2023040 CERN-CZ. We thank Lou-Ann Pestana De Sousa for help with preparation of manuscript.

References

- [1] M. Fisher-Levine and A. Nomerotski, *TimepixCam: a fast optical imager with time-stamping*, *Journal of Instrumentation* **11** (2016) C03016.
- [2] A. Nomerotski, M. Chekhlov, D. Dolzhenko, R. Glazeborg, B. Farella, M. Keach et al., *Intensified Tpx3Cam, a fast data-driven optical camera with nanosecond timing resolution for single photon detection in quantum applications*, *Journal of Instrumentation* **18** (2023) C01023.
- [3] A. Zhao, M. van Beuzekom, B. Bouwens, D. Byelov, I. Chakaberia, C. Cheng et al., *Coincidence velocity map imaging using tpx3cam, a time stamping optical camera with 1.5 ns timing resolution*, *Review of Scientific Instruments* **88** (2017) .
- [4] S.H. Albrechtsen, C.A. Schouder, A. Viñas Muñoz, J.K. Christensen, C. Engelbrecht Petersen, M. Pi et al., *Observing the primary steps of ion solvation in helium droplets*, *Nature* **623** (2023) 319–323.
- [5] E. Sandström, P. Huysmans, F. Giskes, P. Laeven, S. Van Nuffel, R.M.A. Heeren et al., *Improvements in fast mass microscopy for large-area samples*, *Analytical Chemistry* **96** (2024) 18037–18042.
- [6] H. Bromberger, C. Passow, D. Pennicard, R. Boll, J. Correa, L. He et al., *Shot-by-shot 250 kHz 3d ion and mhz photoelectron imaging using timepix3*, *Journal of Physics B: Atomic, Molecular and Optical Physics* **55** (2022) 144001.
- [7] A. Roberts, P. Svihra, A. Al-Refaie, H. Graafsma, J. Küpper, K. Majumdar et al., *First demonstration of 3d optical readout of a TPC using a single photon sensitive timepix3 based camera*, *Journal of Instrumentation* **14** (2019) P06001.
- [8] L.M. Hirvonen, M. Fisher-Levine, K. Suhling and A. Nomerotski, *Photon counting phosphorescence lifetime imaging with timepixcam*, *Review of Scientific Instruments* **88** (2017) 013104.
- [9] R. Sen, L.M. Hirvonen, A. Zhdanov, P. Svihra, S. Andersson-Engels, A. Nomerotski et al., *New luminescence lifetime macro-imager based on a tpx3cam optical camera*, *Biomed. Opt. Express* **11** (2020) 77.
- [10] R. Sen, A.V. Zhdanov, T.F.S. Bastiaanssen, L.M. Hirvonen, P. Svihra, P. Fitzgerald et al., *Mapping o2 concentration in ex-vivo tissue samples on a fast PLIM macro-imager*, *Scientific Reports* **10** (2020) .
- [11] G. D'Amen, M. Keach, A. Nomerotski, P. Svihra and A. Tricoli, *Novel imaging technique for α -particles using a fast optical camera*, *Journal of Instrumentation* **16** (2021) P02006.
- [12] A.S. Losko, Y. Han, B. Schillinger, A. Tartaglione, M. Morgano, M. Strobl et al., *New perspectives for neutron imaging through advanced event-mode data acquisition*, *Scientific Reports* **11** (2021) .
- [13] J. Yang, J. Zhou, X. Jiang, J. Tan, L. Zhang, J. Zhou et al., *A novel energy resolved neutron imaging detector based on a time stamping optical camera for the CSNS*, *Nuclear Instruments and Methods in*

- [14] A. Wolfertz, A. Gustschin, M. Schulz, A.M. Long, A. Khaplanov, T.Y. Hirsh et al., *Lumacam: a novel class of position-sensitive event mode particle detectors using scintillator screens*, *Scientific Reports* **14** (2024) .
- [15] C. Ianzano, P. Svihra, M. Flament, A. Hardy, G. Cui, A. Nomerotski et al., *Fast camera spatial characterization of photonic polarization entanglement*, *Scientific Reports* **10** (2020) .
- [16] Y. Zhang, D. England, A. Nomerotski, P. Svihra, S. Ferrante, P. Hockett et al., *Multidimensional quantum-enhanced target detection via spectrot temporal-correlation measurements*, *Phys. Rev. A* **101** (2020) 053808.
- [17] P. Svihra, Y. Zhang, P. Hockett, S. Ferrante, B. Sussman, D. England et al., *Multivariate discrimination in quantum target detection*, *arXiv:2005.00612* (2020) .
- [18] A. Nomerotski, M. Keach, P. Stankus, P. Svihra and S. Vintskevich, *Counting of Hong-Ou-Mandel Bunched Optical Photons Using a Fast Pixel Camera*, *Sensors* **20** (2020) .
- [19] Y. Zhang, D. England, A. Nomerotski and B. Sussman, *High speed imaging of spectral-temporal correlations in hong-ou-mandel interference*, *Optics Express* **29** (2021) 28217.
- [20] X. Gao, Y. Zhang, A. D'Errico, K. Heshami and E. Karimi, *High-speed imaging of spatiotemporal correlations in hong-ou-mandel interference*, *Optics Express* **30** (2022) 19456.
- [21] Y. Zhang, A. Orth, D. England and B. Sussman, *Ray tracing with quantum correlated photons to image a three-dimensional scene*, *Physical Review A* **105** (2022) .
- [22] L.A. Zhukas, P. Svihra, A. Nomerotski and B.B. Blinov, *High-fidelity simultaneous detection of a trapped-ion qubit register*, *Physical Review A* **103** (2021) .
- [23] L.A. Zhukas, M.J. Millican, P. Svihra, A. Nomerotski and B.B. Blinov, *Direct observation of ion micromotion in a linear paul trap*, *Physical Review A* **103** (2021) .
- [24] A. Kato, A. Goel, R. Lee, Z. Ye, S. Karki, J.J. Liu et al., *Two-tone doppler cooling of radial two-dimensional crystals in a radio-frequency ion trap*, *Physical Review A* **105** (2022) .
- [25] J. Vallerga, A. Tremsin, J. DeFazio, T. Michel, J. Alozy, T. Tick et al., *Optical mcp image tube with a quad timepix readout: initial performance characterization*, *Journal of Instrumentation* **9** (2014) C05055–C05055.
- [26] M. Fiorini, J. Alozy, M. Bolognesi, M. Campbell, A.C. Ramusino, X. LLopart et al., *Single-photon imaging detector with 10 ps timing and sub-10 micron position resolutions*, *Journal of Instrumentation* **13** (2018) C12005–C12005.
- [27] R. Bolzonella, J. Alozy, R. Ballabriga, N. Biesuz, M. Campbell, V. Cavallini et al., *Development and characterization of hybrid mcp-pmt with embedded timepix4 asic used as pixelated anode*, *Nuclear Instruments and Methods in Physics Research Section A: Accelerators, Spectrometers, Detectors and Associated Equipment* **1082** (2026) 170965.
- [28] M. Jachura and R. Chrapkiewicz, *Shot-by-shot imaging of Hong–Ou–Mandel interference with an intensified sCMOS camera*, *Optics letters* **40** (2015) 1540.
- [29] B.M. Jost, A.V. Sergienko, A.F. Abouraddy, B.E. Saleh and M.C. Teich, *Spatial correlations of spontaneously down-converted photon pairs detected with a single-photon-sensitive CCD camera*, *Optics Express* **3** (1998) 81.
- [30] G. Brida, L. Caspani, A. Gatti, M. Genovese, A. Meda and I.R. Berchera, *Measurement of Sub-Shot-Noise Spatial Correlations without Background Subtraction*, *Phys. Rev. Lett.* **102** (2009) 213602.

- [31] L. Zhang, L. Neves, J.S. Lundeen and I.A. Walmsley, *A characterization of the single-photon sensitivity of an electron multiplying charge-coupled device*, *Journal of Physics B: Atomic, Molecular and Optical Physics* **42** (2009) 114011.
- [32] R. Fickler, M. Krenn, R. Lapkiewicz, S. Ramelow and A. Zeilinger, *Real-time imaging of quantum entanglement*, *Scientific reports* **3** (2013) 1914.
- [33] A. Avella, I. Ruo-Berchera, I.P. Degiovanni, G. Brida and M. Genovese, *Absolute calibration of an EMCCD camera by quantum correlation, linking photon counting to the analog regime*, *Optics letters* **41** (2016) 1841.
- [34] M. Reichert, X. Sun and J.W. Fleischer, *Quality of spatial entanglement propagation*, *Physical Review A* **95** (2017) 063836.
- [35] P.-A. Moreau, E. Toninelli, T. Gregory and M.J. Padgett, *Imaging with quantum states of light*, *Nature Reviews Physics* **1** (2019) 367.
- [36] J. Alozy, N. Biesuz, M. Campbell, V. Cavallini, A. Cotta Ramusino, M. Fiorini et al., *Development of a single-photon imaging detector with pixelated anode and integrated digital read-out*, *Journal of Instrumentation* **17** (2022) C06007.
- [37] S. Karl, V. Leopold, S. Richter, Y. Prokazov, E. Turbin, G. Sintotskiy et al., *High-throughput single photon detection for effective stellar intensity interferometry*, in *Advanced Photon Counting Techniques XIX*, M.A. Itzler, K.A. McIntosh and J.C. Bienfang, eds., p. 2, SPIE, May, 2025, DOI.
- [38] E. Charbon, *Single-photon imaging in complementary metal oxide semiconductor processes*, *Philosophical Transactions of the Royal Society A: Mathematical, Physical and Engineering Sciences* **372** (2014) 20130100.
- [39] M. Perenzoni, L. Pancheri and D. Stoppa, *Compact SPAD-based pixel architectures for time-resolved image sensors*, *Sensors* **16** (2016) 745.
- [40] L. Gasparini, B. Bessire, M. Unternährer, A. Stefanov, D. Boiko, M. Perenzoni et al., *SUPERTWIN: towards 100kpixel CMOS quantum image sensors for quantum optics applications*, in *Quantum Sensing and Nano Electronics and Photonics XIV*, vol. 10111, pp. 404–414, SPIE, 2017.
- [41] C. Bruschini, H. Homulle, I.M. Antolovic, S. Burri and E. Charbon, *Single-photon avalanche diode imagers in biophotonics: review and outlook*, *Light: Science & Applications* **8** (2019) 87.
- [42] K. Morimoto, A. Ardelean, M.-L. Wu, A.C. Ulku, I.M. Antolovic, C. Bruschini et al., *Megapixel time-gated SPAD image sensor for 2D and 3D imaging applications*, *Optica* **7** (2020) 346.
- [43] M. Wojtkiewicz, B. Rae and R.K. Henderson, *Review of Back-Side Illuminated 3-D-Stacked SPADs for Time-of-Flight and Single-Photon Imaging*, *IEEE Transactions on Electron Devices* (2024) .
- [44] J. Jirsa, S. Kulkov, R.A. Abrahao, J. Crawford, A. Mueninghoff, E. Bernasconi et al., *Fast data-driven spectrometer with direct measurement of time and frequency for multiple single photons*, *Optics Express* **33** (2025) 9962.
- [45] S. Kulkov, O. Matousek, L.-A.P. De Sousa, L. Radmacherova, D. Sevaev, Y. Kurochkin et al., *Hanbury brown-twiss interference with massively parallel spectral multiplexing for broadband light*, 2025. 10.48550/ARXIV.2509.05649.
- [46] R.H. Hadfield, *Single-photon detectors for optical quantum information applications*, *Nature Photonics* **3** (2009) 696–705.
- [47] P. Seitz and A.J. Theuwissen, *Single-photon imaging*, vol. 160, Springer Science & Business Media (2011).
- [48] A. Nomerotski, *Imaging and time stamping of photons with nanosecond resolution in timepix based optical cameras*, *Nuclear Instruments and Methods in Physics Research Section A: Accelerators, Spectrometers, Detectors and Associated Equipment* **937** (2019) 26.

[49] X. Llopart, J. Alozy, R. Ballabriga, M. Campbell, R. Casanova, V. Gromov et al., *Timepix4, a large area pixel detector readout chip which can be tiled on 4 sides providing sub-200 ps timestamp binning*, *Journal of Instrumentation* **17** (2022) C01044.

[50] K. Heijhoff, K. Akiba, R. Ballabriga, M. van Beuzekom, M. Campbell, A. Colijn et al., *Timing performance of the timepix4 front-end*, *Journal of Instrumentation* **17** (2022) P07006.

[51] T. Poikela, J. Plosila, T. Westerlund, M. Campbell, M.D. Gaspari, X. Llopart et al., *Timepix3: a 65k channel hybrid pixel readout chip with simultaneous toa/tot and sparse readout*, *Journal of Instrumentation* **9** (2014) C05013–C05013.

[52] A. Nomerotski, I. Chakaberia, M. Fisher-Levine, Z. Janoska, P. Takacs and T. Tsang, *Characterization of timepixcam, a fast imager for the time-stamping of optical photons*, *Journal of Instrumentation* **12** (2017) C01017.

[53] B. Winter, S.J. King, M. Brouard and C. Vallance, *A fast microchannel plate-scintillator detector for velocity map imaging and imaging mass spectrometry*, *Review of Scientific Instruments* **85** (2014) .

[54] S. Tsigaridas, M. Beuzekom, H. Graaf, F. Hartjes, K. Heijhoff, N. Hessey et al., *Timewalk correction for the timepix3 chip obtained with real particle data*, *Nuclear Instruments and Methods in Physics Research Section A: Accelerators, Spectrometers, Detectors and Associated Equipment* **930** (2019) 185–190.

[55] R. Bolzonella, J. Alozy, R. Ballabriga, M. van Beuzekom, N. Biesuz, M. Campbell et al., *Timing resolution performance of timepix4 bump-bonded assemblies*, *Journal of Instrumentation* **19** (2024) P07021.

[56] J. Dorkel and P. Leturcq, *Carrier mobilities in silicon semi-empirically related to temperature, doping and injection level*, *Solid-State Electronics* **24** (1981) 821–825.

[57] O. Zapadlík, M. Nikl, J. Polák, P. Průša and V. Linhart, *Engineering of yag:ce to improve its scintillation properties*, *Optical Materials: X* **15** (2022) 100165.

[58] G. Pellegrini, P. Fernández-Martínez, M. Baselga, C. Fleta, D. Flores, V. Greco et al., *Technology developments and first measurements of low gain avalanche detectors (lgad) for high energy physics applications*, *Nuclear Instruments and Methods in Physics Research Section A: Accelerators, Spectrometers, Detectors and Associated Equipment* **765** (2014) 12–16.

[59] A. Doblas, D. Flores, S. Hidalgo, N. Moffat, G. Pellegrini, D. Quirion et al., *Inverse lgad (ilgad) periphery optimization for surface damage irradiation*, *Sensors* **23** (2023) 3450.

[60] P. Svihra, R. Bates, J. Braach, E. Buschmann, D. Dannheim, D. Maneuski et al., *Laboratory and beam-test performance study of a 55 μm pitch ilgad sensor bonded to a timepix3 readout chip*, *Journal of Instrumentation* **19** (2024) C11006.